MAGNETOHYDRODYNAMIC FLOW AND HEAT TRANSFER OF TWO IMMISCIBLE FLUIDS WITH INDUCED MAGNETIC FIELD EFFECTS

by

Živojin M. STAMENKOVIĆ**, Dragiša D. NIKODIJEVIĆ, Miloš M. KOCIĆ, and Jelena D. NIKODIJEVIĆ

Faculty of Mechanical Engineering, University of Niš , Niš , Serbia

Original scientific paper
DOI: 10.2298/TSCI120430172S

The paper investigates the magnetohydrodynamic flow of two immiscible, electrically conducting fluids between isothermal and insulated moving plates in the presence of an applied electric and inclined magnetic field with the effects of induced magnetic field. Partial differential equations governing the flow and heat transfer and magnetic field conservation are transformed to ordinary differential equations and solved exactly in both fluid regions, under physically appropriate boundary and interface conditions. Closed-form expressions are obtained for the non-dimensional velocity, non-dimensional induced magnetic field and non-dimensional temperature. The analytical results for various values of the Hartmann number, the angle of magnetic field inclination, loading parameter and the ratio of plates' velocities are presented graphically to show their effect on the flow and heat transfer characteristics.

Key words: *magnetohydrodynamics, immiscible fluids, moving plates, heat transfer*

Introduction

The interest in the outer magnetic field effect on heat-physical processes appeared seventy years ago. Blum [1] carried out one of the first works in the field of heat and mass transfer in the presence of a magnetic field. The application of magnetohydrodynamic (MHD) flow control in aerospace engineering was already considered in the mid 1950s. This was coincident with the first studies on the problem of an aerospace vehicle reentering the atmosphere from space. The high temperature reached at the surface of the vehicle flying at hypersonic speed causes the ionization of the surrounding air molecules and the consequent formation of a plasma. By imposing a suitable magnetic field, it is possible to modify the aerodynamic forces and heat transfer rates in a convenient way. The increasing interest in the study of MHD phenomena is related to the development of fusion reactors where plasma is confined by a strong magnetic field (Hunt *et al.* [2]). Morley *et al.* [3] studied MHD effects in the so-called blanket. The blanket is located between the plasma and the magnetic field coils, and absorbs neutrons transforming their energy into heat, which is then carried away by a suitable coolant, preventing neutrons from reaching the magnets,

* Corresponding author; e-mail: zikas@masfak.ni.ac.rs

thus avoiding radiation damages. Many exciting innovations have been put forth in the areas of MHD propulsion [4] and remote energy deposition for drag reduction [5]. Double-diffusive MHD convection is significant for material solidification processes [6] and fluid flow over a flat surface or stretching sheet in the presence of a magnetic field finds applications in manufacturing processes such as the cooling of the metallic plate, rolling, purification of molten metals, extrusion of polymers, wire and fiber coating, hydro-magnetic lubrication [7-10]. Extensive research is present in MHD control of flow and heat transfer in the boundary layer [11-14], enhanced plasma ignition [15], and combustion modeling [16]. The analysis of the flow on an inclined porous plate [17] has become the basis of several scientific and engineering applications.

Extensive research has, however, revealed that additional and refined fidelity of physics in modeling and analyzing the interdisciplinary endeavor is required to reach a conclusive assessment. In order to ensure a successful and effective use of electromagnetic phenomena in industrial processes and technical systems, a very good understanding of the effects of the application of a magnetic field to the flow of electrically conducting fluids in channels and various geometric elements is required. With this in mind, most recent research activities tend to refocus on basic and simpler fluid dynamic-electromagnetic interaction phenomena. The application of electromagnetic forces to material processing [18] has been recognized as a promising technology and it is based on the fact that magnetic fields can influence the flow of electrically conducting fluids in different ways. Industrial processes and technical systems where MHD effects are utilized show that the magnetic field represents a versatile and non-intrusive means to control and influence the flow of liquid metals. Therefore, it can be employed to develop new production methods and to improve existing processes to obtain, for instance, high quality materials. All the mentioned studies pertain to a single-fluid model. Most of the problems relating to the petroleum industry, plasma physics, magneto-fluid dynamics, *etc*., involve multi-fluid flow situations. There have been some experimental/analytical studies on hydrodynamic aspects of the two-fluid flow in literature.

Following the ideas of Alireza and Sahai [19], Malashetty *et al.* [20, 21] studied the two fluid MHD flow and heat transfer in an inclined channel, and flow in an inclined channel containing porous and fluid layer. Umavathi *et al.* [22, 23] presented analytical solutions of an oscillatory Hartmann two-fluid flow and heat transfer in a horizontal channel and an unsteady two-fluid flow and heat transfer in a horizontal channel. Recently, Malashetty *et al.* [24] analyzed the problem of magnetoconvection of two-immiscible fluids in vertical enclosure. The above papers about MHD flows analyzed an externally applied magnetic field perpendicular to the flow and ignored magnetic induction effects, which are invoked when the magnetic Reynolds number is non-negligible. To simulate such flows, a separate magnetic field conservation equation has to be solved with appropriate boundary conditions. Several important studies have considered hydromagnetic flow and heat transfer with induced magnetic field effects [25, 26].

Keeping in view the wide area of practical importance of multi-fluid flows and induced magnetic field effects as mentioned, the objective of this study to investigate the MHD flow and heat transfer of two immiscible fluids between moving isothermal and nonconducting plates in the presence of an applied electric field, an inclined externally applied magnetic field, and the effects of an induced magnetic field.

Mathematical model

As mentioned in the introduction, the problem of the MHD two fluid flow between parallel moving plates is considered in this paper. The fluids in the two regions were assumed

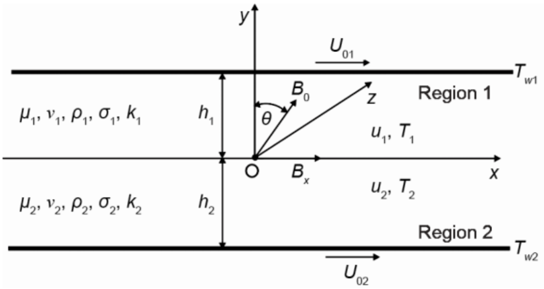

Figure 1. Physical model and co-ordinate system

immiscible and incompressible and the flow was steady, one-dimensional and fully developed. Furthermore, the two fluids had different kinematic viscosities ν_1 and ν_2 and densities ρ_1 and ρ_2. The physical model shown in fig. 1 consists of two infinite parallel plates extending in the x-and z-direction. The upper plate moves with constant velocity U_{01} in the positive longitudinal direction, while the lower plate moves with velocity U_{02} in the same direction. Region 1: $0 \le y \le h_1$ was occupied by a fluid of viscosity μ_1, electrical conductivity σ_1, and thermal conductivity k_1, and region 2: $-h_2 \le y \le 0$ was filled with a layer of different fluid of viscosity μ_2, thermal conductivity k_2 and electrical conductivity σ_2.

A uniform magnetic field of strength B_0 was applied in the direction making an angle θ to the vertical line, and, due to the fluid motion, a magnetic field of the strength B_x was induced along the lines of motion.

The fluid velocity $\vec{\mathrm{v}}$ and the magnetic field distributions are:

$$\vec{\mathrm{v}} = u(y), 0, 0 \tag{1}$$

$$\vec{\mathrm{B}} = \left[B_x(y) + B_0\sqrt{1-\lambda^2}, B_0\lambda, 0 \right] \tag{2}$$

where $\vec{\mathrm{B}}$ is the magnetic field vector and $\lambda = \cos\theta$.

The upper and lower plates were kept at two constant temperatures T_{w1} and T_{w2}, respectively, and the plates were electrically insulated.

The described MHD two fluid flow problem is mathematically presented with a continuity equation:

$$\nabla \cdot \vec{\mathrm{v}} = 0 \tag{3}$$

– momentum equation:

$$\rho\left[\frac{\partial \vec{\mathrm{v}}}{\partial t} + (\vec{\mathrm{v}} \cdot \nabla)\vec{\mathrm{v}}\right] = -\nabla p + \mu\nabla^2\vec{\mathrm{v}} + \vec{\mathrm{J}} \times \vec{\mathrm{B}} \tag{4}$$

– magnetic field conservation equation:

$$\frac{\partial \vec{\mathrm{B}}}{\partial t} - \nabla \times (\vec{\mathrm{v}} \times \vec{\mathrm{B}}) - \frac{1}{\sigma\mu_e}\nabla^2\vec{\mathrm{B}} = 0 \tag{5}$$

– energy equation:

$$\rho c_p\left(\frac{\partial T}{\partial t} + \vec{\mathrm{v}} \cdot \nabla T\right) = k\nabla^2 T + \mu\Phi + \frac{\vec{\mathrm{J}}^2}{\sigma} \tag{6}$$

where

$$\Phi = 2\left[\left(\frac{\partial u}{\partial x}\right)^2 + \left(\frac{\partial v}{\partial y}\right)^2 + \left(\frac{\partial w}{\partial z}\right)^2\right] + \left(\frac{\partial v}{\partial x} + \frac{\partial u}{\partial y}\right)^2 + \left(\frac{\partial w}{\partial y} + \frac{\partial v}{\partial z}\right)^2 + \left(\frac{\partial u}{\partial z} + \frac{\partial w}{\partial x}\right)^2 - \frac{2}{3}(\nabla \cdot \vec{\mathrm{v}})^2 \tag{7}$$

In the previous general equations and in the following boundary conditions, applicable for both fluid regions, the used symbols are common for the theory of MHD flows. The third term on the right hand side of equation (4) is the magnetic body force and $\vec{\mathrm{J}}$ is the current density vector due to the magnetic and electric fields defined by:

$$\vec{\mathrm{J}} = \sigma(\vec{\mathrm{E}} + \vec{\mathrm{v}} \times \vec{\mathrm{B}}) \tag{8}$$

where $\vec{\mathrm{E}}$ = (0, 0, E_z) is the vector of the applied electric field.

Using the velocity, magnetic and electric field distribution as stated above, equation (4) to equation (6) are as follows:

$$\frac{1}{\rho}P + \nu\frac{\mathrm{d}^2 u}{\mathrm{d}y^2} - \frac{\sigma}{\rho}B_0\lambda(E_z + uB_0\lambda) = 0 \tag{9}$$

$$B_0\lambda\frac{\mathrm{d}u}{\mathrm{d}y} + \frac{1}{\sigma\mu_e}\frac{\mathrm{d}^2 B_x}{\mathrm{d}y^2} = 0 \tag{10}$$

$$\rho c_p u\frac{\partial T}{\partial x} = k\frac{\partial^2 T}{\partial y^2} + \mu\left(\frac{\partial u}{\partial y}\right)^2 + \sigma(E_z + uB_0\lambda)^2 \tag{11}$$

where

$$P = -\frac{\partial p}{\partial x} \tag{12}$$

The flow and thermal boundary conditions were unchanged by the addition of electromagnetic fields. The no slip conditions required that the fluid velocities were equal to the plates' velocities and boundary conditions on temperature were isothermal conditions. In addition, the fluid velocity, induced magnetic field, sheer stress and heat flux must be continuous across the interface y = 0. Equations that represent conditions for fluids 1 and 2 are:

$$u_1(h_1) = U_{01},\ u_2(-h_2) = U_{02} \tag{13}$$

$$u_1(0) = u_2(0) \tag{14}$$

$$\mu_1\frac{\mathrm{d}u_1}{\mathrm{d}y} = \mu_2\frac{\mathrm{d}u_2}{\mathrm{d}y},\ y = 0 \tag{15}$$

$$B_{x1}(h_1) = 0,\ B_{x2}(-h_2) = 0 \tag{16}$$

$$B_{x1}(0) = B_{x2}(0) \tag{17}$$

$$\frac{1}{\mu_{e1}\sigma_1}\frac{\mathrm{d}B_{x1}}{\mathrm{d}y} = \frac{1}{\mu_{e2}\sigma_2}\frac{\mathrm{d}B_{x2}}{\mathrm{d}y}\ \text{ for }\ y = 0 \tag{18}$$

$$T_1(0)=T_2(0) \tag{19}$$

$$T_1(h_1)=T_{w1}\,,\ T_2(-h_2)=T_{w2} \tag{20}$$

$$k_1\frac{\mathrm{d}T_1}{\mathrm{d}y}=k_2\frac{\mathrm{d}T_2}{\mathrm{d}y}\,;\ y=0 \tag{21}$$

Velocity and magnetic field distribution

The governing equation for the velocity u_i in regions 1 and 2 can be written as:

$$\frac{1}{\rho_i}P+\nu_i\frac{\mathrm{d}^2u_i}{\mathrm{d}y_i^2}-\frac{\sigma_i}{\rho_i}B_0\lambda(E_z+u_iB_0\lambda)=0 \tag{22}$$

where, suffix i (i = 1,2) represents the values for regions 1 and 2, respectively. The equation for the magnetic field induction in regions 1 and 2 can be written as:

$$B_0\lambda\frac{\mathrm{d}u_i}{\mathrm{d}y_i}+\frac{1}{\sigma_i\mu_{ei}}\frac{\mathrm{d}^2B_{xi}}{\mathrm{d}y_i^2}=0 \tag{23}$$

It is convenient to transform equations (22) and (23) into a non-dimensional form. The following transformations were used:

$$u_i^*=\frac{u_i}{U_{0i}}\,,\ y_i^*=\frac{y_i}{h_i},\ i=1,2 \tag{24}$$

$$\alpha=\frac{\mu_1}{\mu_2}\,,\ \beta=\frac{h_1}{h_2},\ \varepsilon=\frac{U_{01}}{U_{02}},\ \gamma=\frac{\sigma_1}{\sigma_2}\,,\ \delta=\frac{\mu_{e1}}{\mu_{e2}} \tag{25}$$

$$G_i=\frac{P}{\left(\dfrac{\mu_iU_{0i}}{h_i^2}\right)},\ b_i=\frac{B_{xi}}{B_0},\ i=1,2 \tag{26}$$

$$K_i=\frac{E_z}{U_{0i}B_0},\ i=1,2\ \text{– loading parameter} \tag{27}$$

$$\mathrm{Ha_i}=B_0h_i\sqrt{\frac{\sigma_i}{\mu_i}},\ i=1,2\ \text{– Hartmann number} \tag{28}$$

$$\mathrm{Rm_i}=U_{0i}h_i\sigma_i\mu_{ei},\ i=1,2\ \text{– magnetic Reynolds number.} \tag{29}$$

With the non-dimensional quantities, the governing equations become:

$$\frac{\mathrm{d}^2u_i^*}{\mathrm{d}y_i^{*2}}-\mathrm{Ha_i^2}(K_i+u_i^*\lambda)\lambda+G_i=0 \tag{30}$$

$$\frac{\mathrm{d}^2 b_i}{\mathrm{d}y_i^{*2}} + \lambda \mathrm{Rm_i} \frac{\mathrm{d}u_i^*}{\mathrm{d}y_i^*} = 0 \tag{31}$$

The non-dimensional form of the boundary and interface conditions (13) to (18) becomes:

$$u_1^*(1) = 1,\ u_2^*(-1) = 1 \tag{32}$$

$$u_2^*(0) = \varepsilon u_1^*(0) \tag{33}$$

$$\frac{\mathrm{d}u_1^*}{\mathrm{d}y_1^*} = \frac{\beta}{\alpha\varepsilon}\frac{\mathrm{d}u_2^*}{\mathrm{d}y_2^*} \quad \text{for} \quad y_i^* = 0,\ i = 1, 2 \tag{34}$$

$$b_1(1) = 0,\ b_2(-1) = 0 \tag{35}$$

$$b_1(0) = b_2(0) \tag{36}$$

$$\frac{\mathrm{d}b_1}{\mathrm{d}y_1^*} = \beta\gamma\delta\left(\frac{\mathrm{d}b_2}{\mathrm{d}y_2^*}\right) \quad \text{for} \quad y_i^* = 0,\ i = 1, 2 \tag{37}$$

The solutions of eqs. (30) and (31) with boundary and interface conditions have forms:

$$u_i^*(y_i^*) = D_{1i}\cosh(\lambda \mathrm{Ha}_i y_i^*) + D_{2i}\sinh(\lambda \mathrm{Ha}_i y_i^*) + F_i \tag{38}$$

$$b_i(y_i^*) = -\frac{\mathrm{Rm_i}}{\mathrm{Ha_i}}\left[D_{1i}\sinh(\lambda \mathrm{Ha_i} y_i^*) + D_{2i}\cosh(\lambda \mathrm{Ha_i} y_i^*)\right] + Q_{1i} y_i^* + Q_{2i} \tag{39}$$

where

$$F_i = \frac{G_i}{\lambda^2 \mathrm{Ha_i^2}} - \frac{K_i}{\lambda},\ i = 1, 2 \tag{40}$$

$$D_{11} = \frac{H(1 - F_1)\sinh(\lambda \mathrm{Ha}_2) - L\sinh(\lambda \mathrm{Ha}_1)}{W} \tag{41}$$

$$L = F_2 + S\cosh(\lambda \mathrm{Ha}_2) - 1 \tag{42}$$

$$W = H\cosh(\lambda \mathrm{Ha}_1)\sinh(\lambda \mathrm{Ha}_2) + \varepsilon\sinh(\lambda \mathrm{Ha}_1)\cosh(\lambda \mathrm{Ha}_2) \tag{43}$$

$$H = \left(\frac{\alpha\varepsilon}{\beta}\right)\frac{\mathrm{Ha}_1}{\mathrm{Ha}_2} \tag{44}$$

$$S = \frac{1}{\lambda^2}\left(\varepsilon\frac{G_1}{\mathrm{Ha}_1^2} - \frac{G_2}{\mathrm{Ha}_2^2}\right) + \frac{1}{\lambda}(K_2 - \varepsilon K_1) \tag{45}$$

$$D_{21} = \frac{(1 - F_1)\cosh(\lambda \mathrm{Ha}_2) + L\cosh(\lambda \mathrm{Ha}_1)}{W} \tag{46}$$

$$D_{12} = S + D_{11} \tag{47}$$

$$D_{22} = HD_{21} \tag{48}$$

$$Q_{11} = \mathrm{Rm}_1 \lambda D_{11} + \delta\gamma (Q_{12} - \lambda \mathrm{Rm}_2 D_{12}) \tag{49}$$

$$Q_{21} = \frac{\mathrm{Rm}_1}{\mathrm{Ha}_1} \; D_{11} \sinh(\lambda \mathrm{Ha}_1) + D_{21} \cosh(\lambda \mathrm{Ha}_1) \; - Q_{11} \tag{50}$$

$$Q_{12} = \frac{M_1 + M_2}{1 + \delta\gamma} \tag{51}$$

$$M_1 = \frac{\mathrm{Rm}_1}{\mathrm{Ha}_1} \; D_{11} \; \sinh(\lambda \mathrm{Ha}_1) - \lambda \mathrm{Ha}_1 \; + D_{21} \; \cosh(\lambda \mathrm{Ha}_1) - 1 \tag{52}$$

$$M_2 = \frac{\mathrm{Rm}_2}{\mathrm{Ha}_2} \; D_{12} \; \sinh(\lambda \mathrm{Ha}_2) + \lambda\delta\gamma \mathrm{Ha}_2 \; + D_{22} \; 1 - \cosh(\lambda \mathrm{Ha}_2) \tag{53}$$

$$Q_{22} = \frac{\mathrm{Rm}_2}{\mathrm{Ha}_2} \; D_{22} \cosh(\lambda \mathrm{Ha}_2) - D_{12} \sinh(\lambda \mathrm{Ha}_2) \; + Q_{12} \tag{54}$$

Temperature distribution

Once the velocity distributions were known, the temperature distributions for the two regions were determined by solving the energy equation subject to the appropriate boundary and interface conditions (19)-(21). In the present problem, it was assumed that the two plates were maintained at constant temperatures. The term involving $\partial T/\partial x = 0$ in the energy eq. (11) dropped out for such a condition. The governing equation for the temperatures T_1 and T_2 in regions 1 and 2 is then given by:

$$k_i \frac{\mathrm{d}^2 T_i}{\mathrm{d}y_i^2} + \mu_i \left(\frac{\mathrm{d}u_i}{\mathrm{d}y_i} \right)^2 + \sigma_i (E_z + u_i B_0 \lambda)^2 = 0 \tag{55}$$

In order to non-dimensionalize the previous equation, the following transformations were used beside the already introduced (24) to (29):

$$\Theta_i = \frac{T_i - T_{wi}}{\dfrac{U_{0i}^2 \mu_i}{k_i}}, \; \xi = \frac{k_1}{k_2} \tag{56}$$

With the above non-dimensional quantities equation (55) for regions 1 and 2 becomes:

$$\frac{\mathrm{d}^2 \Theta_i}{\mathrm{d}y_i^{*2}} + \left(\frac{\mathrm{d}u_i^*}{\mathrm{d}y_i^*} \right)^2 + Ha_i^2 (K_i + u_i^* \lambda)^2 = 0, \; i = 1,2 \tag{57}$$

In the non-dimensional form, the boundary conditions for temperature and heat flux at the interface $y = 0$ becomes:

$$\Theta_1(1)=0,\ \Theta_2(-1)=0 \tag{58}$$

$$\Theta_1(0)=\left(\frac{\xi}{\varepsilon^2\alpha}\right)\Theta_2(0)+S^* \tag{59}$$

$$S^*=\frac{1}{U_{01}^2}\frac{k_1}{\mu_1}(T_{w2}-T_{w1}) \tag{60}$$

$$\frac{\mathrm{d}\Theta_1}{\mathrm{d}y_1^*}=\frac{\beta}{\alpha\varepsilon^2}\frac{\mathrm{d}\Theta_2}{\mathrm{d}y_2^*},\ y_i^*=0,\ i=1,2 \tag{61}$$

The solution of eq. (57) with boundary and interface conditions has the form:

$$\begin{aligned}\Theta_i(y_i^*)=-\frac{1}{4\lambda}\Big[&\lambda(D_{1i}^2+D_{2i}^2)\cosh(2\lambda\mathrm{Ha}_i y_i^*)+8D_{2i}C_i\sinh(\lambda\mathrm{Ha}_i y_i^*)+\\&+2D_{1i}D_{2i}\lambda\sinh(2\lambda\mathrm{Ha}_i y_i^*)+8D_{1i}C_i\cosh(\lambda\mathrm{Ha}_i y_i^*)-\\&-2\lambda(2D_{3i}+2D_{4i}y_i^*-\mathrm{Ha}_i{}^2C_i^2y_i^{*2})\Big]\end{aligned} \tag{62}$$

where

$$C_i=K_i+\lambda F_i=\frac{G_i}{\lambda\mathrm{Ha}_i^2},\ i=1,2 \tag{63}$$

$$D_{31}=\frac{\xi}{\alpha\varepsilon^2}D_{42}+\frac{\xi}{\alpha\varepsilon^2}\Im_2+\Im_3 \tag{64}$$

$$D_{41}=\frac{\beta}{\alpha\varepsilon^2}D_{42}+\Im_4 \tag{65}$$

$$D_{32}=D_{42}+\Im_2 \tag{66}$$

$$D_{42}=\frac{\alpha\varepsilon^2}{\xi+\beta}\left(\Im_1-\frac{\xi}{\alpha\varepsilon^2}\Im_2-\Im_3-\Im_4\right) \tag{67}$$

$$\begin{aligned}\Im_1=\frac{1}{4\lambda}\Big[&\lambda(D_{11}^2+D_{21}^2)\cosh(2\lambda\mathrm{Ha}_1)+8D_{21}C_1\sinh(\lambda\mathrm{Ha}_1)+\\&+2D_{11}D_{21}\lambda\sinh(2\lambda\mathrm{Ha}_1)+8D_{11}C_1\cosh(\lambda\mathrm{Ha}_1)+2\lambda\mathrm{Ha}_1{}^2C_1^2\Big]\end{aligned} \tag{68}$$

$$\begin{aligned}\Im_2=\frac{1}{4\lambda}\Big[&\lambda(D_{12}^2+D_{22}^2)\cosh(2\lambda\mathrm{Ha}_2)-8D_{22}C_2\sinh(\lambda\mathrm{Ha}_2)-\\&-2D_{12}D_{22}\lambda\sinh(2\lambda\mathrm{Ha}_2)+8D_{12}C_2\cosh(\lambda\mathrm{Ha}_2)+2\lambda\mathrm{Ha}_2{}^2C_2^2\Big]\end{aligned} \tag{69}$$

$$\Im_3 = \frac{1}{4}\left[D_{11}^2 + D_{21}^2 - \frac{\xi}{\alpha\varepsilon^2}(D_{12}^2 + D_{22}^2)\right] + \frac{2}{\lambda}\left(D_{11}C_1 - \frac{\xi}{\alpha\varepsilon^2}D_{12}C_2\right) + S^* \tag{70}$$

$$\Im_4 = D_{21}(2C_1 + \lambda D_{11})\mathrm{Ha}_1 - \frac{\beta}{\alpha\varepsilon^2}D_{22}(2C_2 + \lambda D_{12})\mathrm{Ha}_2 \tag{71}$$

Results and discussion

In this section, the results for steady MHD flow and heat transfer of two immiscible fluids between moving plates are presented and discussed for various parametric conditions. In order to show the results of the considered flow problem graphically, two fluids important for technical practice are chosen and the parameters α, β, ξ, and γ take the values of 0.678, 1, 0.0647, and 0.025, respectively. The part of obtained results is presented graphically in fig. 2 to fig. 13 to elucidate the significant features of the hydrodynamic and thermal state of the flow.

The fig. 2 to fig. 4 show the effect of the magnetic field inclination angle on the distribution of velocity, temperature and the ratio of the applied and induced magnetic field.

Figure 2 shows the effect of the angle of inclination on velocity which predicts that the velocity increases as the inclination angle increases. These results are expected because the application of a transverse magnetic field normal to the flow direction has a tendency to create a drag-like Lorentz force which has a decreasing effect on the flow velocity.

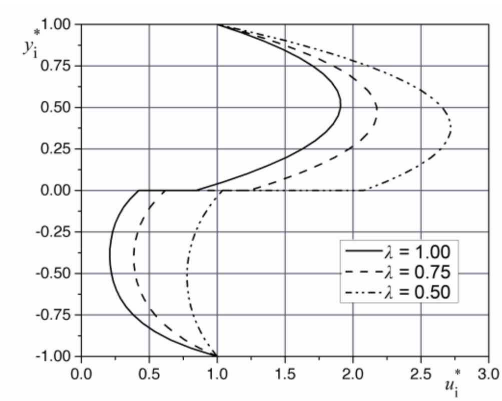

Figure 2. Velocity profiles for different values of magnetic field inclination angle
$\mathrm{Ha}_1 = 1$, $\mathrm{Ha}_2 = 5$, $K_i = 0$, $\varepsilon = 0.5$

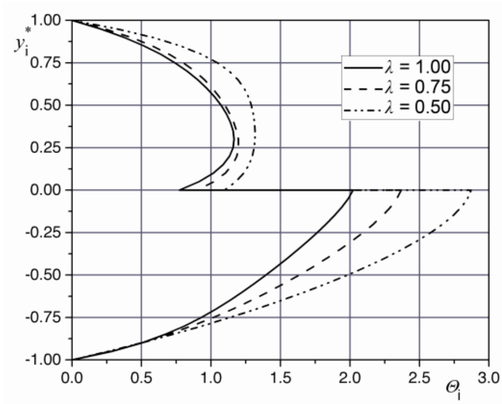

Figure 3. Temperature profiles for different values of magnetic field inclination angle
$\mathrm{Ha}_1 = 1$, $\mathrm{Ha}_2 = 5$, $K_i = 0$, $\varepsilon = 0.5$

Figures 2 and 3 show an unusual jump of dimensionless velocity and temperature at the interface which results from choice of u_i^* and Θ_i, and not from the physical properties of flow (temperature and velocity are continuous across the interface). It can be seen from fig. 2 and fig. 3 that the magnetic field flattens out the velocity and temperature profiles in region 1 and reduces the flow energy transformation as the inclination angle decreases.

Figure 4 shows that the ratio of an induced and externally imposed magnetic field increases as the inclination angle of an applied field decreases. In the observed case for negative values of y_i^* this ratio has a tendency to move the maximum value closer to the lower plate while λ decreases. The obtained results show that the magnetic induction can be strongly controlled, for example, in an MHD induction generator system, by adjusting the angle of inclination of the applied magnetic field. The induced magnetic field effect is more obvious in region 2 occupied with the fluid with greater electro conductivity, and the fact that magnetic induction will vanish at some distance from the lower plate is also of significance in the optimized operation of MHD induction devices.

Figures 5 to 7 depict the effect of the Hartmann number, while the electric loading factor K_i is equal to zero (so-called short-circuited case). The influence of the Hartmann number on the velocity profiles was more pronounced in channel region 2 containing the fluid with greater electrical conductivity. Figure 5 illustrates the effect of the Hartmann number on the velocity field. It was found that for large values of Hartmann number the flow could be almost completely stopped in region 2, while in region 1 the velocity decrease was significant. The effect of the Hartmann number increase on the temperature profiles (fig. 6) in both of the parallel-plate channel regions was manifested in equalizing the fluid temperatures.

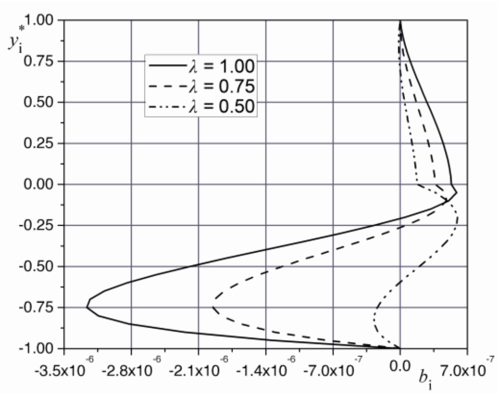

Figure 4. Ratio of an induced and externally imposed magnetic field
$Ha_1 = 1$, $Ha_2 = 5$, $K_i = 0$, $\varepsilon = 0.5$

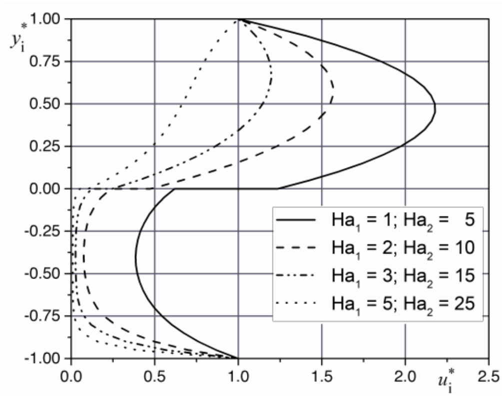

Figure 5. Velocity profiles for different values of Hartmann numbers
$\lambda = 0.75$, $K_i = 0$, $\varepsilon = 0.5$

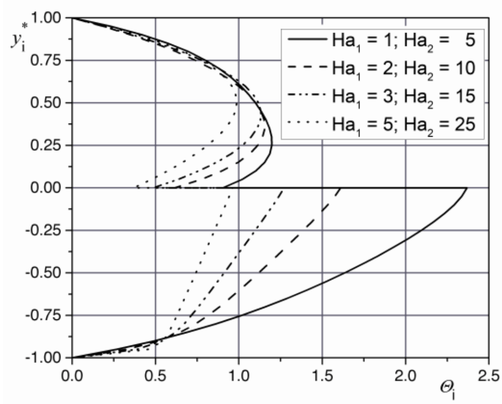

Figure 6. Temperature profiles for different values of Hartmann numbers
$\lambda = 0.75$, $K_i = 0$, $\varepsilon = 0.5$

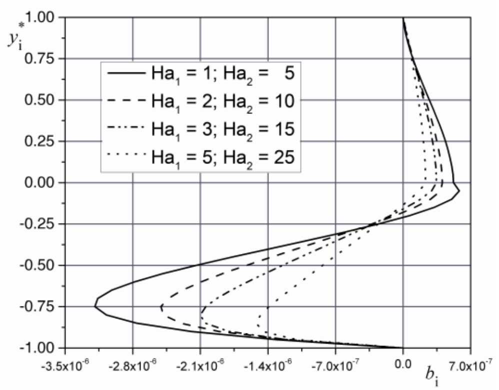

Figure 7. Ratio of an induced and externally imposed magnetic field
$\lambda = 0.75$, $K_i = 0$, $\varepsilon = 0.5$

The influence of the Hartmann number on the ratio of induced and externally applied magnetic field is shown in fig. 7. Magnetic induction is evidently suppressed with an increase in the applied magnetic field, *Ha*; however, closer to the lower plate the magnitudes of B_x remain negative; further from the plate they decrease and become positive near to the interface.

Of particular significance is the analysis when the loading factor K_i is different from zero (the value of loading factor K_i defines the system as generator, flowmeter or pump). Figure 8 illustrates that with the increase of loading factor K_i the temperature in regions 1 and 2 increases. The effect of the decrease in loading factor K_i results in equalizing of temperature fields in regions 1 and 2.

Figure 9 shows the effect of the loading factor on velocity, which predicts the possibility to change the flow direction, although the plates move in the same direction. For negative K_i values, the flow rate increases. The obtained results show that different values of the inclination angle, the Hartmann number, and the loading factor are a convenient control method for heat and mass transfer processes.

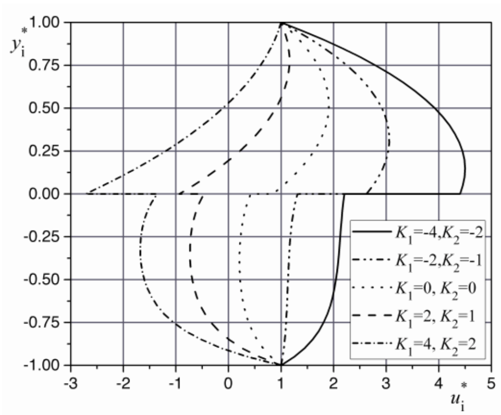

Figure 8. Velocity profiles for different values of loading factor
$Ha_1 = 1$, $Ha_2 = 5$, $\lambda = 1$, $\varepsilon = 0.5$

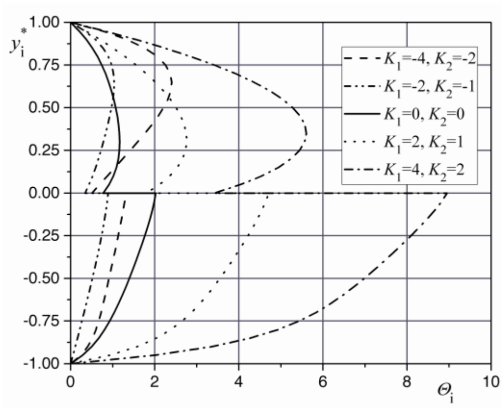

Figure 9. Temperature profiles for different values of loading factor
$Ha_1 = 1$, $Ha_2 = 5$, $\lambda = 1$, $\varepsilon = 0.5$

Figure 10 shows the change of induced field as a function of loading factor. The ratio of an induced and externally imposed magnetic field had a considerable change when the loading parameter was different from zero, especially in region 2. Figure 10 also shows a direction change of the induced field in regions 1 and 2.

Close to the lower plate, the values of B_x are negative/positive (for positive/negative values of K_i); however, B_x changes the sign close to the interface. The absolute value of the induced magnetic field increases with the increase in the loading parameter. Further from the lower plate (region 2 containing the fluid with greater electrical conductivity) *i. e.* in the free stream, the induced magnetic field again vanishes, and obtains some small positive or negative value at the interface.

The effect of the plates' velocities ratio on the velocity field is shown in fig.11. It is interesting to note that decreasing ε increases the velocity. The effect of the plates' velocities ratio on the temperature field is the opposite compared to the effect on the velocity field, which is evident from fig. 12. It was found that the effect of decreasing ε was a decrease in the temperature field in regions 1 and 2. It is also interesting to note that for small ε, the ratio of induced and externally imposed magnetic field became negligibly small in region 1, as shown in fig. 13. Increasing of ε changed this ratio considerably in region 2, while the ratio stayed nearly the same in region 1.

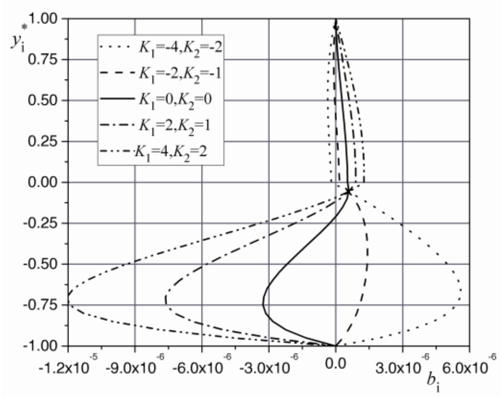

Figure 10. Ratio of an induced and externally imposed magnetic field for different values of loading factor
$\mathrm{Ha}_1 = 1$, $\mathrm{Ha}_2 = 5$, $\lambda = 1$, $\varepsilon = 0.5$

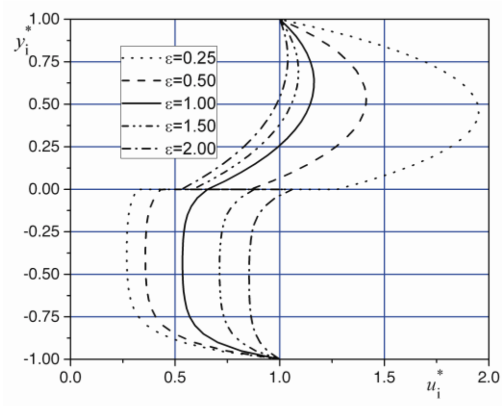

Figure 11. Velocity profiles for different values of plates velocities ratio
$\mathrm{Ha}_1 = 2$, $\mathrm{Ha}_2 = 10$, $\lambda = 1$, $K_1 = 0.5$

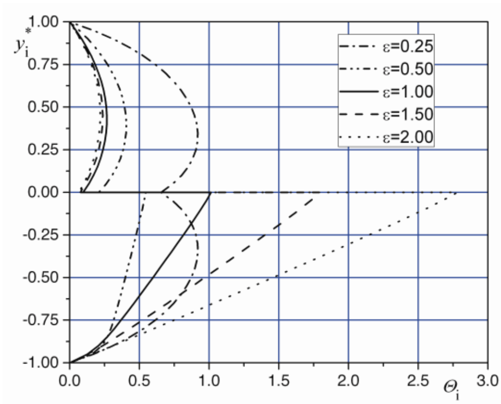

Figure 12. Temperature profiles for different values of plates' velocities ratio ε,
$\mathrm{Ha}_1 = 2$, $\mathrm{Ha}_2 = 10$, $\lambda = 1$, $K_1 = 0.5$

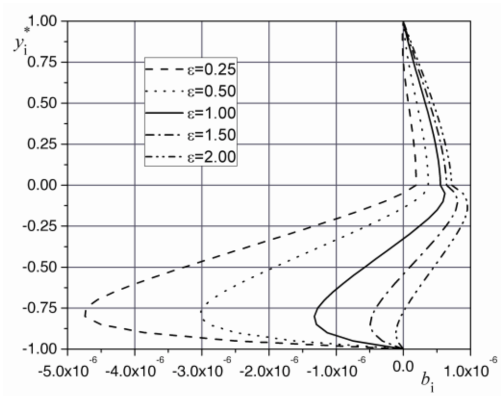

Figure 13. Ratio of an induced and externally imposed magnetic field for different values of ε,
$\mathrm{Ha}_1 = 2$, $\mathrm{Ha}_2 = 10$, $\lambda = 1$, $K_1 = 0.5$

Conclusions

The problem of MHD flow and heat transfer of two immiscible fluids between moving parallel plates in the presence of applied electric and inclined magnetic fields was investigated analytically. Both fluids were assumed Newtonian and electrically conducting. Closed form solutions for dimensionless velocity, temperature and magnetic induction of each fluid were obtained taking into consideration suitable interface matching conditions and boundary conditions. The results were numerically evaluated and presented graphically for two fluids important for technical practice. Only the part of the results is presented for various values of the magnetic field inclination angle, Hartmann number, loading parameter and plates' velocities ratio. The obtained results show that the control of flow and heat transfer for the observed case can be realized by changing the magnetic field inclination angle, the Hartmann number, the loading factor, and the ratio of plates' velocities.

Acknowledgments

This paper is supported by the Serbian Ministry of Sciences and Technological Development (Project No. TR 35016; Research of MHD flow in the channels, around the bodies and application in the development of the MHD pump).

Nomenclature

$\vec{B}$ – magnetic field vector, [T]
B_0 – strength of applied magnetic field, [T]
B_x – strength of induced magnetic field, [T]
b_i – dimensionless ratio of magnetic fields
c_p – specific heat capacity, [$\mathrm{Jkg^{-1}K^{-1}}$]
C_i – constants
D_{ij} – constants
$\vec{E}$ – electric field vector, [$\mathrm{Vm^{-1}}$]
F_i – constants
Ha_i – Hartmann number in region i
h_j – region i height, [m]
$\vec{J}$ – current density vector, [$\mathrm{Am^{-2}}$]
K_i – load factor in region i
k_i – thermal conductivity in region i, [$\mathrm{WK^{-1}m^{-1}}$]
L – constant
M_i – constants
p – pressure, [Pa]
Q_{ij} – constants
Rm_i – magnetic Reynolds number in region i
S – constant
T – temperature, [K]
t – time, [s]
U_{0i} – absolute velocity of plates, [$\mathrm{ms^{-1}}$]
u_i – fluid velocity in region i, [$\mathrm{ms^{-1}}$]
$\vec{V}$ – velocity vector, [$\mathrm{ms^{-1}}$]
x – longitudinal coordinate, [m]
y – transversal coordinate, [m]
W – constant

Greek symbols

α – viscosities ratio of fluids
β – ratio of region heights
δ – ratio of magnetic permeability's
γ – ratio of electrical conductivities
ε – ratio of plates velocities
Φ – dissipative function
λ – cosine of inclination angle θ
μ_i – dynamic viscosity in region i, [$\mathrm{kgm^{-1}s^{-1}}$]
μ_{ei} – magnetic permeability in region i, [$\mathrm{Hm^{-1}}$]
ν_i – kinematic viscosity in region i, [$\mathrm{m^2s^{-1}}$]
θ – magnetic filed inclination angle [$^\mathrm{o}$]
Θ_i – dimensionless temperature in region i
ρ_i – density of fluid in region i, [$\mathrm{kgm^{-3}}$]
σ_i – electrical conductivity region i, [$\mathrm{Sm^{-1}}$]
ξ_i – ratio of thermal conductivities
$\mathfrak{I}_i$ – constants

References

[1] Blum, Ya. E., Heat and Mass Transfer in Magnetic Field, *Magnetohydrodynamics*, *11* (1967), 1, pp. 27-36
[2] Hunt, J. C., Holroyd, R. J., Applications of Laboratory and Theoretical MHD Duct Flow Studies in Fusion Reactor Technology, Technical Report CLM-R169, Culham Laboratory, Oxfordshire, UK, 1977
[3] Morley, N. B. *et al*., Thermofluid Magnetohydrodynamic Issues for Liquid Breeders, *Fusion Science and Technology, 47* (2005), pp. 488-501
[4] Davidson P. A., Pressure Forces in the MHD Propulsion of Submersibles, *Magnetohydrodynamics*, *29,* (1993), 3, pp. 49-58
[5] Tsinober, A., MHD-Drag Reduction, in: Viscous Drag Reduction in Boundary Layers, *AIAA Progress in Aeronautics and Astronautics, 123* (1990), pp. 327-349
[6] Younsi, R., Computational Analysis of MHD Flow, Heat and Mass Transfer in Trapezoidal Porous Cavity, *Thermal Science*, *13* (2009), 1, pp. 13-22
[7] Mohamed, A. A., Flow and Heat Transfer over an Unsteady Stretching Surface with Hall Effect, *Meccanica*, *45* (2010), 1, pp. 97-109
[8] Sharma, P. R., Singh, G., Effects of Ohmic Heating and Viscous Dissipation on Steady MHD Flow Near a Stagnation Point on an Isothermal Stretching Sheet, *Thermal Science*, *13* (2009), 1, pp. 5-12

[9] Vadher P. A. *et al*., Performance of Hydromagnetic Squeeze Films between Conducting Porous Rough Conical Plates, *Meccanica*, *45* (2010), 6, pp. 767-783
[10] Kumar, H., Radiative Heat Transfer with Hydromagnetic Flow and Viscous Dissipation over a Stretching Surface in the Presence of Variable Heat Flux, *Thermal Science*, *13* (2009), 2, pp. 163-169
[11] Boričić, Z. *et al*., Universal Equations of Unsteady Two-Dimensional MHD Boundary Layer whose Temperature Varies with Time, *Theoretical and Applied Mechanics*, *36* (2009), 2, pp. 119-135
[12] Obrović, B. *et al*., Boundary Layer of Dissociated Gas on Bodies of Revolution of a Porous Contour, *Strojniški vestnik - Journal of Mechanical Engineering*, *55* (2009), 4, pp. 244-253
[13] Xu, H. *et al*., Series Solutions of Unsteady Three-Dimensional MHD Flow and Heat Transfer in the Boundary Layer over an Impulsively Stretching Plate, *European Journal of Mechanics B/Fluids*, *26* (2007), 1, pp. 15-27
[14] Boričić, Z. *et al*., Universal Solutions of Unsteady Two-Dimensional MHD Boundary Layer on the Body with Temperature Gradient along Surface, *WSEAS Transactions on Fluid Mechanics*, *4* (2009), 3, pp. 97-106
[15] Kessel, C. E. *et al*., Physics Basis and Simulation of Burning Plasma Physics for the Fusion Ignition Research Experiment (FIRE), *Fusion Engineering and Design*, *63-64* (2002), pp. 559-567
[16] Pesochin V. R. Acoustic Instability while Combusting Aluminum Particles in MHD Facilities, *Doklady Physics*, *47* (2002), 3, pp. 215-218
[17] Sharma P. R., Singh G., Effects of Variable Thermal Conductivity, Viscous Dissipation on Steady MHD Natural Convection Flow of Low Prandtl Fluid on an Inclined Porous Plate with Ohmic Heating, *Meccanica*, *45* (2010), 2, pp. 237-247
[18] Davidson, P. A., Magnetohydrodynamics in Materials Processing, *Annual Review of Fluid Mechanics*, *31* (1999), pp. 273-300
[19] Alireza, S., Sahai, V., Heat Transfer in Developing Magnetohydrodynamic Poiseuille Flow and Variable Transport Properties, *International Journal of Heat and Mass Transfer*, *33* (1990), 8, pp. 1711-1720
[20] Malashetty, M. S. *et al*., Convective MHD Two Fluid Flow and Heat Transfer in an Inclined Channel, *Heat and Mass Transfer*, *37* (2001), 2-3, pp. 259-264
[21] Malashetty, M. S. *et al*., Two Fluid Flow and Heat Transfer in an Inclined Channel Containing Porous and Fluid Layer, *Heat and Mass Transfer*, *40* (2004), 11, pp. 871-876
[22] Umavathi, J. C. *et al*., Oscillatory Hartmann Two-Fluid Flow and Heat Transfer in a Horizontal Channel, *International Journal of Applied Mechanics and Engineering*, *11* (2006), 1, pp. 155-178
[23] Umavathi, J. C. *et al*., Unsteady Two-Fluid Flow and Heat Transfer in a Horizontal Channel, *Heat and Mass Transfer*, *42* (2005), 2, pp. 81-90
[24] Malashetty, M. S., Umavathi, J. C., Kumar, J. P., Magnetoconvection of Two Immiscible Fluids in Vertical Enclosure, *Heat and Mass Transfer*, *42* (2006), pp. 977-993
[25] Ghosh, S. K. *et al*., Hydromagnetic Free Convection Flow with Induced Magnetic Field Effects, *Meccanica*, *45* (2010), 2, pp. 175-185
[26] Bég, O. A. *et al*., Nonsimilar, Laminar, Steady, Electrically-Conducting Forced Convection Liquid Metal Boundary Layer Flow with Induced Magnetic Field Effects, *International Journal of Thermal Science*, *48* (2009), 8, pp. 1596-1606

Paper submitted: April 30, 2012
Paper revised: June 20, 2012
Paper accepted: June 29, 2012